

## DEMONSTRATION OF MUON ACCELERATION AND CAVITY DESIGN OF THE MUON LINAC FOR J-PARC E34

M. Otani, T. Mibe, M. Yoshida, KEK, Tsukuba, Japan  
N. Saito, J-PARC/KEK, Tokai, Japan  
R. Kitamura, The University of Tokyo, Tokyo, Japan  
Y. Iwashita, KUICR, Kyoto University, Kyoto, Japan  
Y. Kondo, J-PARC/JAEA, Tokai, Japan

### Abstract

We are developing a linac dedicated to the muon acceleration. It enables us to measure the muon anomalous magnetic moment with an accuracy of 0.1 ppm and search for the muon electric dipole moment with a sensitivity of  $10^{-21} \text{ e} \cdot \text{cm}$  to explore beyond Standard Model of elementary particle physics. As a first step for demonstration of the muon acceleration, we are developing the source of slow muons with which RFQ acceleration is conducted. In order to cover the middle beta ( $\beta \sim 0.3 - 0.7$ ) section of the muon LINAC, disk and washer coupled cell LINAC is employed and the DAW cell being designed now. This paper describes status of these developments.

### INTRODUCTION

Though the discovery of Higgs at LHC completed the particles predicted in Standard Model (SM) of elementary particle physics, some observations such as dark matter existence indicate new physics beyond SM at some energy scale or interaction scale. One of the clues for new physics is anomaly of the muon anomalous magnetic moment  $(g - 2)_\mu$ ; There is a  $\sim 3 \sigma$  discrepancy between the SM prediction and the experimental value measured by E821 with a precision of 0.54 ppm [1]. Measurement with higher precision (0.1 ppm) is necessary to confirm this anomaly.

It should be also noted that measurements up to now rely on the technique of the magic momentum. Because the muon beam generated from the secondary pions in flight has large emittance, focusing with the electric field in addition to the magnetic field is necessary in the storage ring. The spin precession vector of muon is written by

$$\vec{\omega} = -\frac{e}{m} \left[ a_\mu \vec{B} - \left( a_\mu - \frac{1}{\gamma^2 - 1} \right) \frac{\vec{\beta} \times \vec{E}}{c} + \frac{\eta}{2} \left( \vec{\beta} \times \vec{B} + \frac{\vec{E}}{c} \right) \right] \quad (1)$$

where  $e$  is the elementary charge,  $m$  is the muon mass,  $a_\mu$  is the anomalous magnetic moment,  $\gamma$  is the Lorentz Factor,  $\beta$  is the ratio of particle velocity to the speed of light  $c$ , and  $\eta$  is the electric dipole moment. The second term depending on the electric field is eliminated when the muon momentum is 3.094 GeV/c, so called magic momentum. Measurement with a new method should be surveyed for verification of the  $(g - 2)_\mu$  anomaly.

The muon electric dipole moment (EDM) is also sensitive to new physics because it is strongly suppressed in SM ( $10^{-38} \text{ e} \cdot \text{cm}$ ), and violates CP symmetry assuming the CPT theorem.

In addition to that, there is a possibility that anomaly of  $(g - 2)_\mu$  can be explained by finite EDM with an order of  $10^{-20} \text{ e} \cdot \text{cm}$  [2], whereas current direct limit is  $1.9 \times 10^{-19} \text{ e} \cdot \text{cm}$  [3].

The E34 experiment [4] aims to measure  $(g - 2)_\mu$  with a precision of 0.1 ppm and search for EDM with a sensitivity to  $10^{-21} \text{ e} \cdot \text{cm}$  by utilizing high intensity proton beam at J-PARC and newly developed novel technique of the ultra-cold muon beam. Figure 1 shows the experimental setup. The experiment utilizes the proton beam from the 3 GeV Synchrotron ring to Materials and Life Science facility (MLF). The proton beam is injected to the graphite target. The generated surface muons are extracted to one of the muon beamline of H-line. Surface muons stop in the muonium ( $\mu^+ e^-$ , Mu) production target of the silica aerogel and then form thermal muoniums. The paired electron in the muonium is knocked out by laser and thermal muon (3 keV/c) is generated. Then the muon is accelerated up to 300 MeV/c and injected to the storage ring supplying 3 T. The decay positron is detected by the silicon strip tracker and the spin precession frequency is obtained from variation of counting rate of the decay positron.

Thanks to the ultra-cold beam ( $\sigma_{pT}/p = 10^{-5}$ ) where  $p_T$  is the transverse momentum of the beam particles, the electric focusing is not necessary anymore. Eq. 1 becomes

$$\vec{\omega} = -\frac{e}{m} \left[ a_\mu \vec{B} + \frac{\eta}{2} (\vec{\beta} \times \vec{B}) \right] \quad (2)$$

Because the anomalous magnetic moment and EDM are perpendicular each other, these can be measured simultaneously.

One of the milestones for the experiment is verification of the muon acceleration, which will be the first case in the world. To suppress muon loss in the acceleration, the muon should be accelerated in a sufficiently short period. To realize the fast acceleration, a linac dedicated to the muon is being developed [5]. Figure 2 shows conceptual design of the muon LINAC. The slow muons are generated in the electric potential of 5.6 keV which corresponds to the input energy of radio-frequency quadrupole (RFQ). The spare for the J-PARC LINAC RFQ, so called RFQ II [6,7], will be used for the muon LINAC. After RFQ, Interdigital H-type (IH) DTL will be used to accelerate muon from  $\beta = 0.08$  to 0.27. Then disk and washer (DAW) coupled cavity is employed to  $\beta = 0.7$  and then disk loaded structure accelerates muons up to 212 MeV/c.

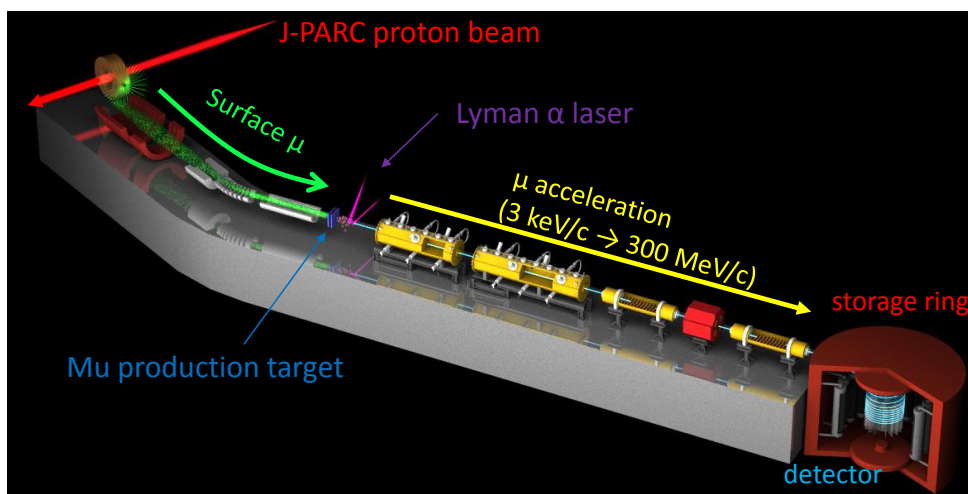


Figure 1: Schematic view of E34.

As a demonstration of the muon acceleration, we are planning to accelerate muons with electro-static field and RFQ II. Next section describes development of the muon source and RFQ for that test. Following section shows current status of the following RF cavity design, especially for DAW. Development of the RF cavity for low and high  $\beta$  section can be found elsewhere [8, 9]. Other experimental developments such as decay positron detector can be found on [10–12].

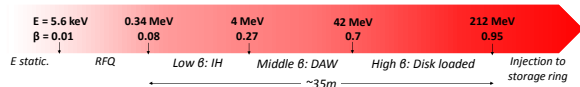


Figure 2: Conceptual design of the muon LINAC.

## MUON ACCELERATION WITH RFQ

In order to conduct muon acceleration with RFQ, slow muon source is being developed. One of the promising candidates is negative muonium ( $\mu^+e^-e^-$ ,  $\text{Mu}^-$ ) or slow muon emission by injecting the surface muon beam to a thin metal foil. Previous experiment observed  $\text{Mu}^-$  and slow muon emission from an Al foil [13] with average energy of  $0.2 \pm 0.1$  keV and few keV, respectively, which can be injected to the RFQ II whose injection energy is 5.6 keV.

The measurement of the  $\text{Mu}^-$  or slow muon emission efficiency and its kinematics was proposed and approved in J-PARC MLF. Figure 3 shows the experimental setup of the measurement. Surface muons are injected into the  $\text{Mu}^-$  production target. The emitted  $\text{Mu}^-$  is accelerated and focused by the electro-static lens and transported to the detector chamber by following electro-static quadrupoles and electro-static deflector. The Micro-Channel-Plate (MCP) [14, 15] is used for counting and timing measurement of  $\text{Mu}^-$  and surrounding plastic scintillators for the decay-positron detection.

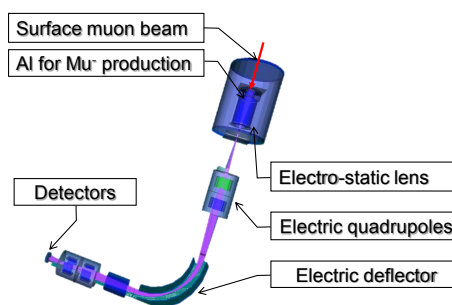


Figure 3: Experimental setup for the  $\text{Mu}^-$  emission measurement at the J-PARC MLF muon beamline.

Figure 4 shows expected MCP timing distribution estimated by the GEANT4 simulation. In the simulation, the  $\text{Mu}^-$  signals are generated at the  $\text{Mu}^-$  target with kinetic energy of 0.2 keV and beam related backgrounds are estimated by injecting the beam muons towards the target. Backgrounds mainly consist of decay-positrons from the beam muons stopped around the target and the deflector, which can be reduced effectively by lead shields around the target chamber and the collimator located on downstream of the deflector. The signal to background ratio is estimated to be more than ten and clear separation between these can be achieved by observed timing as shown in Fig. 4.

The slow muon beamline has been assembled in J-PARC MLF. It was originally developed and operated in RIKEN-RAL port-3 [16]. It successfully demonstrated transportation of the slow muon beam. After shutdown of the beamline, some of the beamline components were moved to J-PARC for the  $\text{Mu}^-$  measurement in summer 2014. Assembly and commissioning of all the equipments were completed by May 2015 as shown in Fig. 5. Figure 6 shows one of the commissioning results of the beamline; an Al plate installed at the  $\text{Mu}^-$  target holder location is irradiated by UV light and then generated photo-electrons are accelerated and trans-

PASJ2015 WEOM02

ported to the MCP detector location. The photo-electron events are observed successfully with nominal setup of the beamline components. Though current setup for  $\text{Mu}^-$  suffers background due to the field emission electrons from the electro-static lens electrodes, the setup for slow muon setup can be operated stably. Upgrade such as a magnetic equipment installation to separate the field emission electron from  $\text{Mu}^-$  is being discussed.

In conclusion, all the equipments are ready for slow muon measurement.

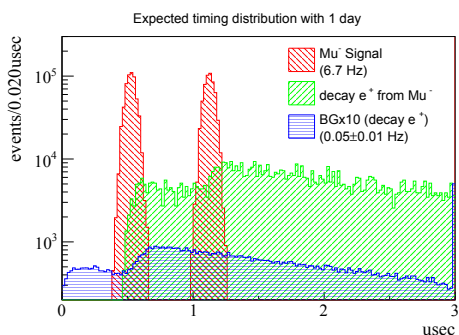


Figure 4: Expected timing distribution estimated by the GEANT4 simulation.

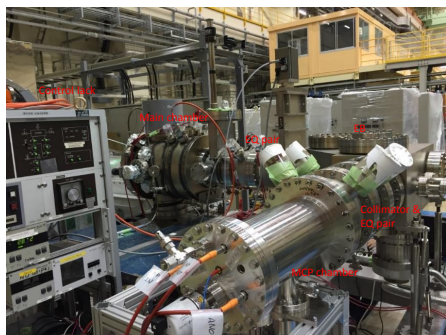


Figure 5:  $\text{Mu}^-$  beamline assembly.

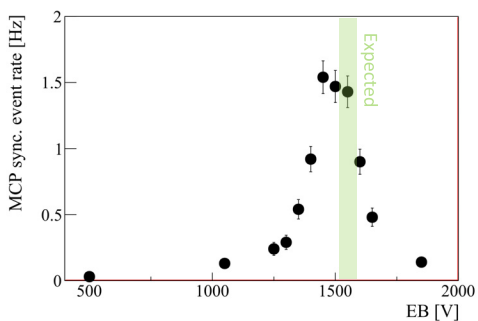


Figure 6: Result of the beamline commissioning. Horizontal axis is set voltage of the electro-static bending apparatus and vertical axis is number of observed events by the MCP detector. Number of events has maximum at expected value from accelerated energy.

In order to verify the RFQ II operation and measure the background from the RF field with MCP, the RFQ offline test was performed in June 2015 in the J-PARC LINAC building.

Figure 7 shows photo of the RFQ offline test setup. The MCP detector chamber is connected to the RFQ downstream. Vacuuming is done with an ion pump and reach  $10^{-6}$  Pa. Figure 8 shows the RFQ operation setup. The RFQ is powered on by low RF source and solid state amplifier up to 6 kW and 25 Hz repetition. The forward, reflection waves and RFQ internal power are monitored by power meters.

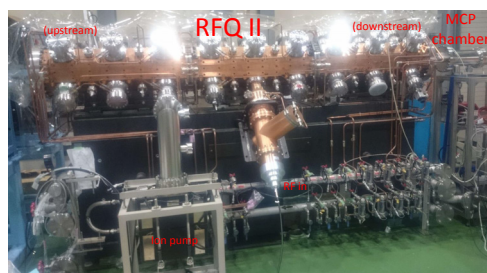


Figure 7: Photo of the RFQ offline test at the J-PARC LINAC building.

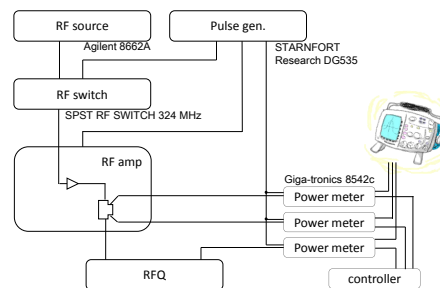


Figure 8: Setup of the RFQ operation.

Figure 9 shows frequency dependence of the forward and reflection power and its ratio. The measured value is well consistent with designed value and previous measurement. Figure 10 shows the forward, reflection and pick-up power in RFQ with nominal power (5 kW) operation. Rising time is well consistent with expectation from Q factor. Figure 11 shows result of the MCP background measurement. Because the slow muon beam intensity in the first stage of the acceleration test is expected to be several counts per second, it is necessary to measure background level with comparable accuracy to that. Though it was expected that there might be background events due to electron or X-ray excited by RF field, all the measurements are consistent each other within statistical error of about 0.1 Hz and no background events are observed.

In conclusion, RFQ is successfully operated and accelerated muons can be measured by MCP without beam related background.

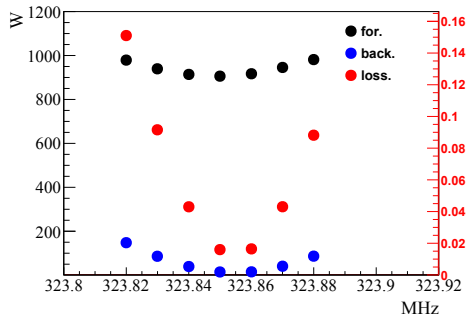


Figure 9: Forward and reflection power as a function of input wave frequency.

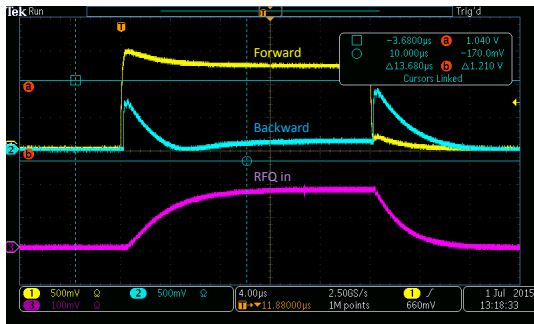


Figure 10: Forward, reflection wave and pick-up power in RFQ with nominal power of 5 kW.

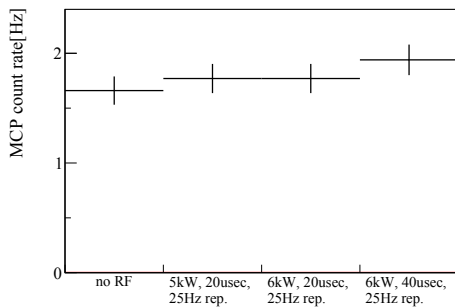


Figure 11: Result of the MCP background measurement. All the measurements are consistent each other within statistical error.

## DEVELOPMENT OF THE MIDDLE $\beta$ SECTION

In the middle beta section ( $\beta = 0.3 \sim 0.7$ ), the DAW cavity will be employed [17]. It has high effective shunt impedance and high degree of coupling between adjacent RF cells. In order to solve the mode overlapping problem, a bi-periodic L-support structure is employed [18].

It is necessary to design our DAW cavity because muon acceleration is the first time in the world and the DAW cavity covering such a wide range of velocity is also the first time. In order to achieve higher acceleration gradient, the cavity design is optimized as follows. First, two dimensional model without the washer supports as shown in Fig. 12 is op-

timized by calculating acceleration and coupling mode with SUPERFISH. Variable parameters are disk radius ( $T_d$ ), disk thickness ( $T_d$ ), washer radius ( $R_w$ ) and gap between washer ( $G$ ) as shown in red characters in Fig. 12. Optimization process is done by the SIMPLEX algorithm and the optimization function is constructed with confluent condition ( $f_a = f_b$ ), higher shunt impedance ( $Z_{TT}$ ), and uniformity of the acceleration field. After optimization in two dimensional model three dimensional model with the washer supports is constructed based on the optimized dimensions with the 2-D code, with which resonant modes around operation frequency of 1.3 GHz are calculated in CST MICROWAVE STUDIO. Here the connection radius of the supports is decided to be the zero-electric point to minimize perturbation to the accelerating mode. In addition, the disk radius with and without the supports are slightly modified to recover the periodic feature of the acceleration field. The three dimensional model is also optimized by using same optimization function as two dimensional one. Finally the dispersion curve is investigated to check whether unfavored mode exists or not around the operation frequency. All the steps are repeated in several cavity lengths of  $\beta\lambda/4$ .

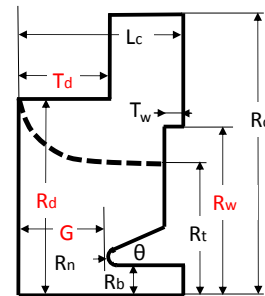


Figure 12: Two dimensional model of the DAW cavity and notations of the dimensions. Red characters are variable parameters in the optimization process.

Figure 13, Fig. 14 and Tab. 1 show the dispersion curve, optimized model and optimized parameters, respectively, with  $\beta = 0.3, 0.4, 0.5$  and  $0.6$ . Because of bi-periodic structure, some stop bands appear in  $\pi/2$ . Though TM11 mode is near to the operational frequency, the cavity is tuned in the optimization process so that the operational frequencies sit in the stop band at  $\pi/2$ . Though the dipole mode passband TE11 crossed the line where the phase velocity matches the speed of muons, it is considered to be no problem because the muon beam current is negligibly small and transverse kick due to this mode is estimated to be much smaller than our requirement.

In conclusion, we completed design of the DAW cavity based on computer calculator. We are planning to fabricate a cold model made by Al and measure resonant frequencies and fields to confirm the calculation result.

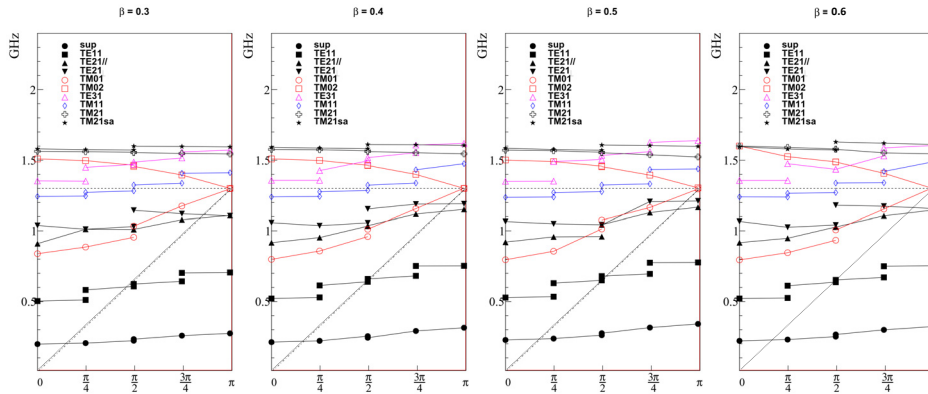


Figure 13: Dispersion curve with optimized cavity in several  $\beta$  calculated by CST MICROWAVE STUDIO.

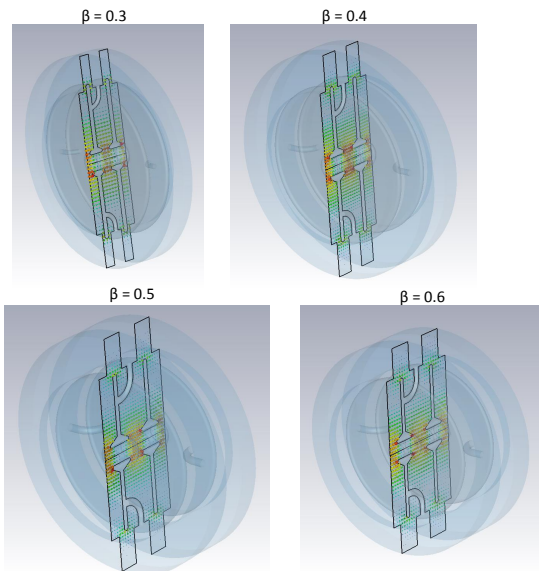


Figure 14: Optimized three dimensional models in CST MICROWAVE STUDIO.

## SUMMARY

Muon acceleration is required for precision measurement of muon g-2 and EDM with ultra-cold muon beam. We are ready for demonstration of muon acceleration with RFQ; slow muon beamline has been completed and RFQ II is available in J-PARC. Design of the DAW cavity has been completed and cold model measurement is planned. The E34 collaboration submitted Technical Design Report and aims to start physics data taking in 2019.

## ACKNOWLEDGMENT

It is a pleasure to thank MLF Muon Section people for helping assembly of the slow muon beamline. We would like to thank J-PARC LINAC group for RFQ offline test. This work was supported by JSPS KAKENHI Grant Numbers 25800164, 15H03666.

Table 1: Parameters of the Optimized DAW Cavity.

$\beta$	0.3	0.4	0.5	0.6
L	$\beta\lambda/4$			
$R_b$ [mm]	12			
$R_n$ [mm]	2.6			
$T_w$ [mm]	3.5			
$\theta$ [deg.]	30			
$R_c$ [mm]	155	157	154	151
$R_d$ [mm]	111.3	108.352	104.52	103.221
$T_d$ [mm]	16.014	14.790	10.97	9.630
$R_w$ [mm]	105.969	105.63	108.14	110.391
G[mm]	15.975	11.285	7.8976	6.148
$f_a$ [GHz]	1.300	1.300	1.299	1.301
$f_c$ [GHz]	1.299	1.301	1.302	1.301
ZTT[M $\Omega$ /m]	57.8	46.3	33.8	18.0

## REFERENCES

- [1] G.W. Bennett et al.: Phys. Rev. **D73** (2006) 072003.
- [2] J.L. Feng et al.: Nucl. Phys. **B613** (2001) 366.
- [3] G.W. Bennett et al.: Phys. Rev. **D80** (2009) 052008.
- [4] J-PARC E34 conceptual design report (2011).
- [5] M. Otani et al.: Proc. of IPAC2015, WEPWA023 (2015).
- [6] Y. Kondo et al.: Phys. Rev. ST Accel. Beams 16. 040102 (2013).
- [7] Y. Kondo et al.: Proc. of IPAC2015, THPF045 (2015).
- [8] K. Saito, Master Thesis, Tokyo Tech., (2012).
- [9] M. Yoshida, Proceedings for IPAC 2015.
- [10] M. Otani for the E34 collaboration, Proceedings for the J-PARC symposium 2014.
- [11] S. Nishimura for the E34 collaboration, Proceedings for the J-PARC symposium 2014.
- [12] G.A. Beer et al.: Prog. Theor. Exp. Phys., **091** (2014) C01.
- [13] Phys. Rev. A39. 6109.
- [14] [http://www.hamamatsu.com/resources/pdf/etd/MCPassy\\_TMCP0001E.pdf](http://www.hamamatsu.com/resources/pdf/etd/MCPassy_TMCP0001E.pdf)

- [15] R. Kitamura, Master Thesis, Tokyo Univ., (2014).
- [16] NIM **B266** (2008) 335.
- [17] M. Otani et al., PASJ **2014** (2014) SAP039.
- [18] Hiroyuki Ao et al., Jpn. J. Appl. Phys. Vol. 39 (2000) 651-656.